Comparisons between 1D and 2D formulations for thin-walled structure analysis

Erasmo Carrera, Maria Cinefra, Marco Petrolo, Enrico Zappino
Department of Aeronautics and Space Engineering, Politecnico di Torino, Italy
E-mail: erasmo.carrera@polito.it, maria.cinefra@polito.it, marco.petrolo@polito.it, enrico.zappino@polito.it

Keywords: Unified Formulation, Shell, Beam.

SUMMARY. The present paper compares 1D and 2D assumptions in the analysis of thin-walled structures. Refined beam/plate/shell models are exploited and the orders of these models are taken as free parameters, that is, classical beam/plate/shell theories can be refined at any extent. Finite Element (FE) approximations are used to handle different boundary conditions (geometrical and mechanical). The Carrera Unified Formulation (CUF) is adopted in order to write finite element matrices of 1D and 2D models (both plate/curved cases) in a concise form based on the so-called fundamental nuclei. Well established benchmark problems which are often used to assess shell problems are solved by implementing both 1D and 2D assumptions. Comparisons between 1D and 2D models are carried out in terms of accuracy and computational costs. Results obtained suggest that 1D CUF models are able to detect shell-like solutions with lower computational costs and less implementation issues.

1 INTRODUCTION

Theory of structures (TOS) can be built according to various methods. If only displacement variables are considered, the fundamental problem of TOS will consist of the evaluation of the minimum number of unknown variables (UVs) needed to solve a given problem according to a fixed accuracy. In the development of the so-called axiomatic approach to TOS, the UVs are introduced by postulating an expansion for the three unknown displacements. Such an expansion can be formulated in many different ways. The generic displacement component u in an orthogonal reference system (x, y, z) can be expanded in terms of one-dimensional (1D) or two-dimensional (2D) UVs, respectively,

$$\begin{aligned} 1D: u = u_i^{1D}(y)\ F_i^{1D}(x,z), \qquad i = 1,..,M_{1D} \\ 2D: u = u_i^{2D}(x,y)\ F_i^{2D}(z), \qquad i = 1,...,M_{2D} \end{aligned} \tag{1}$$

where $u_i^{1D}(y)$ and $u_i^{2D}(x,y)$ are the UVs , F_i^{1D} and F_i^{2D} are the base functions used for the 1D and 2D expansions. It is assumed that in the 1D case the expansion is made in terms of the two coordinates x, z (over a given section for a given z-value) while the expansion is made in terms of z (over the thickness at a given point of coordinates x, y) for 2D models. The base functions can be represented by any kind of polynomials, such as powers of z (or x, z in the 1D cases), harmonics, Lagrange, Legendre, etc. The Principle of Virtual Displacements can be used to derive governing equations (in both weak and strong forms) consistent to the assumptions made in Eq. 1.

This paper is devoted to the analysis of shell structures by means of 1D and 2D structural models. 1D theories are usually referred to as 'beam' models. Most known examples are the Euler-Bernoulli [1] and Timoshenko [2] models. These models are hereafter referred to as EBBT and TBT, respectively. These models provide reliable results if compact structures made of isotropic materials are considered in bending. Higher-order beam models are needed to account for non-classical effects due to, for instance, thin walls or point loads. An excellent review on higher-order models can be found in Kapania and Raciti [3]. 2D shell models may be classified in two classes according to different physical assumptions. The Koiter model [4] is based on the Kirchhoff hypothesis. The Naghdi model [5] is based on the Reissner-Mindlin

assumptions that take into account the transverse shear deformation. It is known that when a finite element method is used to discretize a physical model, the phenomenon of numerical *locking* may arise from hidden constrains that are not well represented in the finite element approximation. There are many approaches proposed to overcome the locking phenomenon, such as the use of the standard displacement formulation with higher-order elements (see [6],[7]), the use of reduced-selective integration techniques (see [8],[9]) or the use of modified variational forms (see [10, 11]).
Numerical examples are herein carried out by using 1D and shell models derived from the Carrera Unified Formulation (CUF) [12]. In the CUF framework, higher-order structural models are obtained hierarchically since the order of the model is considered as an input of the analysis. A cylindrical shell finite element based on CUF [13] is adopted in this paper. In the wake of Bathe et al. [14, 15], the Mixed Interpolation of Tensorial Components (MITC) method has been extended to shell elements with nine nodes in order to overcome the membrane and shear locking. The performances of this element have been tested in [16] by solving discriminating problems from the literature, that involve very thin shells.
1D Taylor-based (TE) models [17] are also exploited. CUF 1D models are able to predict accurate displacement and stress fields of arbitrary shaped and constrained structures [18, 19, 20, 21, 22, 23, 24] with considerable reductions of computational costs.
This paper gives a brief theoretical overview of both 1D and 2D CUF models and then presents the numerical results related to the Scordelis-Lo barrel vault problem.

2 CARRERA UNIFIED FORMULATION

In the CUF framework, the displacement field of a structural model is the expansion of generic functions F_τ,

$$\mathbf{u} = F_\tau \mathbf{u}_\tau, \qquad \tau = 1, 2, ..., M \tag{2}$$

where $\mathbf{u}_\tau$ is the displacement vector and M stands for the number of terms of the expansion. According to the Einstein notation, the repeated subscript, τ, indicates summation. The expression given by Eq. 2 is valid for both 1D and 2D models since these models are obtained by acting on the expansion functions F_τ. In fact,

$$\begin{array}{ll} 1D: & \mathbf{u}(x,y,z) = F_\tau(x,z)\mathbf{u}_\tau(y), \qquad \tau = 1, 2, ..., M_{1D} \\ 2D: & \mathbf{u}(x,y,z) = F_\tau(z)\mathbf{u}_\tau(x,y), \qquad \tau = 1, 2, ..., M_{2D} \end{array} \tag{3}$$

As far as 1D models are concerned, the expansions of the displacement filed are in terms of the cross-section coordinates (x, z) while the unknowns of the problem are given in a certain location above the cross-section. In the case of 2D models, the expansions are in terms of the thickness coordinate (z) and the unknowns are given in a certain point along z.
The choice of F_τ determines the class of CUF models to adopt. Taylor-like polynomial expansions, $x^i\ z^j$ (1D) and z^j (2D), of the displacement fields are adopted in this paper (i and j are positive integers). A generic N-order displacement field for a 1D model is then expressed by:

$$\mathbf{u} = \sum_{N_i=0}^{N} \left(\sum_{M_{1D}=0}^{N_i} x^{N-M_{1D}}\ z^{M_{1D}}\ \mathbf{u}_{\frac{N(N+1)+M_{1D}+1}{2}} \right) \tag{4}$$

For example, the second-order model, TE2, has the following kinematic model:

$$\begin{array}{l} u_x = u_{x_1} + x\ u_{x_2} + z\ u_{x_3} + x^2\ u_{x_4} + xz\ u_{x_5} + z^2\ u_{x_6} \\ u_y = u_{y_1} + x\ u_{y_2} + z\ u_{y_3} + x^2\ u_{y_4} + xz\ u_{y_5} + z^2\ u_{y_6} \\ u_z = u_{z_1} + x\ u_{z_2} + z\ u_{z_3} + x^2\ u_{z_4} + xz\ u_{z_5} + z^2\ u_{z_6} \end{array} \tag{5}$$

The 1D model described by Eq. 5 has 18 generalized displacement variables: three constant, six linear, and nine parabolic terms. The order N of the expansion is arbitrary and is set as an input of the analysis.

The choice of N for a given structural problem is usually made through a convergence study.
If 2D models are considered, a generic Taylor-like displacement field is given by

$$\mathbf{u} = z^{\tau-1}\mathbf{u}_\tau, \qquad \tau = 1, 2, ..., M_{2D} \tag{6}$$

A second-order model (ESL2) is then based on the following displacement field:

$$\begin{array}{l} u_x = u_{x_1} + z\ u_{x_2} + z^2\ u_{x_3} \\ u_y = u_{y_1} + z\ u_{y_2} + z^2\ u_{y_3} \\ u_z = u_{z_1} + z\ u_{z_2} + z^2\ u_{z_3} \end{array} \tag{7}$$

A brief description of the 1D and 2D CUF models will be given hereafter.

2.1 *1D CUF finite elements*

The transposed displacement vector is defined as

$$\mathbf{u}(x, y, z) = \left\{ \begin{array}{ccc} u_x & u_y & u_z \end{array} \right\}^T \tag{8}$$

where x, y, and z are orthonormal axes as shown in Fig. 1. The cross-section of the structure is Ω, the

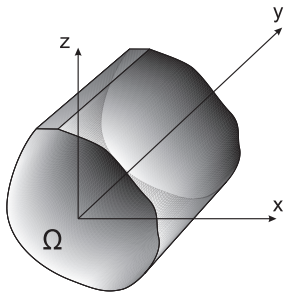

Figure 1: Coordinate frame

longitudinal axis is $0 \leq y \leq L$. Stress, $\boldsymbol{\sigma}$, and strain, $\boldsymbol{\epsilon}$, components are grouped as

$$\begin{array}{ll} \boldsymbol{\sigma}_p = \left\{ \begin{array}{ccc} \sigma_{zz} & \sigma_{xx} & \sigma_{zx} \end{array} \right\}^T, & \boldsymbol{\epsilon}_p = \left\{ \begin{array}{ccc} \epsilon_{zz} & \epsilon_{xx} & \epsilon_{zx} \end{array} \right\}^T \\ \boldsymbol{\sigma}_n = \left\{ \begin{array}{ccc} \sigma_{zy} & \sigma_{xy} & \sigma_{yy} \end{array} \right\}^T, & \boldsymbol{\epsilon}_n = \left\{ \begin{array}{ccc} \epsilon_{zy} & \epsilon_{xy} & \epsilon_{yy} \end{array} \right\}^T \end{array} \tag{9}$$

The subscript "n" stands for terms lying on the cross-section, while "p" stands for terms lying on planes which are orthogonal to Ω.
Strains are obtained as

$$\begin{array}{l} \boldsymbol{\epsilon}_p = \boldsymbol{D}_p\mathbf{u} \\ \boldsymbol{\epsilon}_n = \boldsymbol{D}_n\mathbf{u} = (\boldsymbol{D}_{np} + \boldsymbol{D}_{ny})\mathbf{u} \end{array} \tag{10}$$

where $\boldsymbol{D}_p$ and $\boldsymbol{D}_n$ are differential operators whose explicit expressions is not reported here for the sake of brevity, they can be found in [20]. Constitutive laws are introduced to obtain stress components,

$$\boldsymbol{\sigma} = \tilde{\boldsymbol{C}}\boldsymbol{\epsilon} \tag{11}$$

According to Eq.s 9, the previous equation becomes:

$$\begin{array}{l} \boldsymbol{\sigma}_p = \tilde{\boldsymbol{C}}_{pp}\boldsymbol{\epsilon}_p + \tilde{\boldsymbol{C}}_{pn}\boldsymbol{\epsilon}_n \\ \boldsymbol{\sigma}_n = \tilde{\boldsymbol{C}}_{np}\boldsymbol{\epsilon}_p + \tilde{\boldsymbol{C}}_{nn}\boldsymbol{\epsilon}_n \end{array} \tag{12}$$

where $\tilde{\boldsymbol{C}}_{pp}$, $\tilde{\boldsymbol{C}}_{pn}$, $\tilde{\boldsymbol{C}}_{np}$, and $\tilde{\boldsymbol{C}}_{nn}$ are the material coefficient matrices whose explicit expressions are not reported here for the sake of brevity, they can be found in [20]. The FE approach is herein adopted to discretize the structure along the y-axis, this process is conducted via a classical finite element technique where the displacement vector is given by

$$\mathbf{u}_\tau = N_i F_\tau \mathbf{q}_{\tau i} \tag{13}$$

Where N_i stands for the shape functions and $\mathbf{q}_{\tau i}$ for the nodal displacement vector,

$$\mathbf{q}_{\tau i} = \left\{ \begin{array}{ccc} q_{u_{x_{\tau i}}} & q_{u_{y_{\tau i}}} & q_{u_{z_{\tau i}}} \end{array} \right\}^T \tag{14}$$

Elements with four nodes, hereinafter referred as B4, are formulated, that is, a cubic approximation along the y axis is adopted.
The stiffness matrix of the elements are obtained via the Principle of Virtual Displacements,

$$\delta L_{int} = \int_V (\delta \boldsymbol{\epsilon}_p^T \boldsymbol{\sigma}_p + \delta \boldsymbol{\epsilon}_n^T \boldsymbol{\sigma}_n) dV = \delta L_{ext} \tag{15}$$

Where L_{int} stands for the strain energy and L_{ext} is the work of the external loadings. δ stands for the virtual variation. In a compact notation the stiffness matrix for a given material property set can be written as

$$\begin{aligned} \boldsymbol{K}^{ij\tau s} \;=\; & I_l^{ij} \triangleleft \left(\boldsymbol{D}_{np}^T F_\tau \boldsymbol{I}\right) \Big[\tilde{\boldsymbol{C}}_{np} \left(\boldsymbol{D}_p F_s \boldsymbol{I}\right) \,+\, \tilde{\boldsymbol{C}}_{nn} \left(\boldsymbol{D}_{np} F_s \boldsymbol{I}\right) \Big] + \\ & \left(\boldsymbol{D}_p^T F_\tau \boldsymbol{I}\right) \Big[\tilde{\boldsymbol{C}}_{pp} \left(\boldsymbol{D}_p F_s \boldsymbol{I}\right) \,+\, \tilde{\boldsymbol{C}}_{pn} \left(\boldsymbol{D}_{np} F_s \boldsymbol{I}\right) \Big] \triangleright_\Omega \,+ \\ & I_l^{ij,_y} \triangleleft \Big[\left(\boldsymbol{D}_{np}^T F_\tau \boldsymbol{I}\right) \tilde{\boldsymbol{C}}_{nn} \,+\, \left(\boldsymbol{D}_p^T F_\tau \boldsymbol{I}\right) \tilde{\boldsymbol{C}}_{pn} \Big] F_s \triangleright_\Omega \boldsymbol{I}_{\Omega\, y} + \\ & I_l^{i,_y j} \boldsymbol{I}_{\Omega\, y} \triangleleft F_\tau \Big[\tilde{\boldsymbol{C}}_{np} \left(\boldsymbol{D}_p F_s \boldsymbol{I}\right) \,+\, \tilde{\boldsymbol{C}}_{nn} \left(\boldsymbol{D}_{np} F_s \boldsymbol{I}\right) \Big] \triangleright_\Omega \,+ \\ & I_l^{i,_y j,_y} \boldsymbol{I}_{\Omega\, y} \triangleleft F_\tau \tilde{\boldsymbol{C}}_{nn} F_s \triangleright_\Omega \boldsymbol{I}_{\Omega\, y} \end{aligned} \tag{16}$$

where

$$\boldsymbol{I}_{\Omega\, y} \,=\, \begin{bmatrix} 0 & 1 & 0 \\ 1 & 0 & 0 \\ 0 & 0 & 1 \end{bmatrix} \qquad\qquad \triangleleft \ldots \triangleright_\Omega \,=\, \int_\Omega \ldots \, d\Omega \tag{17}$$

$$\left(I_l^{ij},\, I_l^{ij,_y},\, I_l^{i,_y j},\, I_l^{i,_y j,_y}\right) \,=\, \int_l \Big(N_i\, N_j,\; N_i\, N_{j,_y},\; N_{i,_y}\, N_j,\; N_{i,_y}\, N_{j,_y} \Big)\, dy \tag{18}$$

$\mathbf{K}^{ij\tau s}$ is the stiffness matrix in the form of the fundamental nucleus, its components can be found in [24]. As far as the formal expression of the fundamental nucleus is concerned, it has to be underlined that

- It does not depend on the expansion order.
- It does not depend on the choice of the F_τ expansion polynomials.

These are the key-point of CUF which permits, with only nine FORTRAN statements, to implement any-order multiple class theories.

2.2 *CUF Shell finite element with cylindrical geometry*

In this work a shell element with exact cylindrical geometry is considered. Using the linear part of the 3D Green-Lagrange tensor as shown in [14], one can obtain the following strain-displacement relations expressed in the curvilinear reference system (ξ_1, ξ_2, ξ_3):

$$
\begin{aligned}
\varepsilon_{11} &= F_\tau u_{\tau,1} \\
\varepsilon_{22} &= F_\tau \Big[(1+\frac{\xi_3}{R})\frac{w_\tau}{R} + (1+\frac{\xi_3}{R}) v_{\tau,2} \Big] \\
\varepsilon_{12} &= F_\tau \Big[u_{\tau,2} + (1+\frac{\xi_3}{R}) v_{\tau,1} \Big] \\
\varepsilon_{13} &= w_{\tau,1} F_\tau + u_\tau F_{\tau,3} \\
\varepsilon_{23} &= F_\tau \Big[w_{\tau,2} - \frac{v_\tau}{R} \Big] + F_{\tau,3} \Big[(1+\frac{\xi_3}{R}) v_\tau \Big] \\
\varepsilon_{33} &= w_\tau F_{\tau,3}
\end{aligned}
\tag{19}
$$

where R is the radius of the cylinder taken in the ξ_2-direction (see Fig. 2). The Unified Formulation has

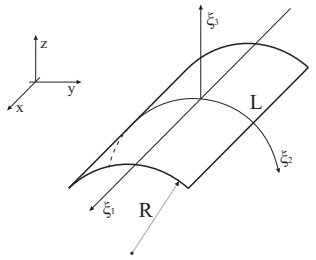

Figure 2: Curvilinear coordinates reference system.

been applied to the displacements. The comma indicates the derivative with respect to the coordinates ξ_1, ξ_2 or ξ_3.
For convenience, the geometrical relations can be expressed in matrix form as:

$$
\begin{aligned}
\boldsymbol{\varepsilon}_p &= (\boldsymbol{D}_p + \boldsymbol{A}_p)\boldsymbol{u} \\
\boldsymbol{\varepsilon}_n &= (\boldsymbol{D}_{n\Omega} + \boldsymbol{D}_{nz} - \boldsymbol{A}_n)\boldsymbol{u}
\end{aligned}
\tag{20}
$$

where the strains have been arranged in the vectors $\boldsymbol{\varepsilon}_p = \{\varepsilon_{11}, \varepsilon_{22}, \varepsilon_{12}\}$ and $\boldsymbol{\varepsilon}_n = \{\varepsilon_{13}, \varepsilon_{23}, \varepsilon_{33}\}$, and the differential operators are defined as follows:

$$
\boldsymbol{D}_p = \begin{bmatrix} \partial_1 & 0 & 0 \\ 0 & H\partial_2 & 0 \\ \partial_2 & H\partial_1 & 0 \end{bmatrix} , \quad \boldsymbol{D}_{n\Omega} = \begin{bmatrix} 0 & 0 & \partial_1 \\ 0 & 0 & \partial_2 \\ 0 & 0 & 0 \end{bmatrix} , \quad \boldsymbol{D}_{nz} = \partial_3 \cdot \boldsymbol{A}_{nz} = \partial_3 \begin{bmatrix} 1 & 0 & 0 \\ 0 & H & 0 \\ 0 & 0 & 1 \end{bmatrix} , \tag{21}
$$

$$
\boldsymbol{A}_p = \begin{bmatrix} 0 & 0 & 0 \\ 0 & 0 & \frac{1}{R}H \\ 0 & 0 & 0 \end{bmatrix} , \boldsymbol{A}_n = \begin{bmatrix} 0 & 0 & 0 \\ 0 & \frac{1}{R} & 0 \\ 0 & 0 & 0 \end{bmatrix} , \tag{22}
$$

in which $H = (1 + \frac{\xi_3}{R})$ and the matrix $\boldsymbol{A}_{n_z}$ is introduced. For more details about the derivation of the geometrical relations one can refer to [14],[16]. According to the FEM, the displacement components can be interpolated on the nodes of the element by means of the Lagrangian shape functions N_i as follows:

$$
\delta \boldsymbol{u}_\tau = N_i \delta \boldsymbol{q}_{\tau_i} , \qquad \boldsymbol{u}_s = N_j \boldsymbol{q}_{s_j} , \tag{23}
$$

where $i, j = 1, ..., 9$ by considering a nine-node element. $\boldsymbol{q}_{s_j}$ and $\delta\boldsymbol{q}_{\tau_i}$ are the nodal displacement components and their virtual variations. Therefore, substituting these expressions in the geometrical relations (20), one has:

$$\begin{aligned}\boldsymbol{\varepsilon}_p =& F_\tau(\boldsymbol{D}_p + \boldsymbol{A}_p)(N_i\boldsymbol{I})\boldsymbol{q}_{\tau_i}\\ \boldsymbol{\varepsilon}_n =& F_\tau(\boldsymbol{D}_{n\Omega} - \boldsymbol{A}_n)(N_i\boldsymbol{I})\boldsymbol{q}_{\tau_i} + F_{\tau,3}\boldsymbol{A}_{nz}(N_i\boldsymbol{I})\boldsymbol{q}_{\tau_i}\end{aligned} \tag{24}$$

where $\boldsymbol{I}$ is a 3×3 identity matrix. The Mixed Interpolation of Tensorial Components (MITC) method is used to contrast the membrane and shear locking phenomenon that affects the shell finite elements. Considering the strains in the local coordinate system (ξ, η), the MITC shell elements ([25],[26]) are formulated by using, instead of the strain components directly computed from the displacements, an interpolation of these strain components within each element using a specific interpolation strategy for each component. The corresponding interpolation points, called tying points, are shown in Fig. 3 for a nine-nodes element.

The interpolating functions on tying points can be arranged in the following arrays:

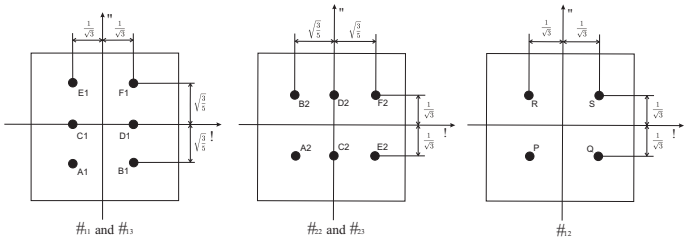

Figure 3: Interpolation strategy for strain components.

$$\begin{aligned}N_{m1} &= [N_{A1}, N_{B1}, N_{C1}, N_{D1}, N_{E1}, N_{F1}]\\ N_{m2} &= [N_{A2}, N_{B2}, N_{C2}, N_{D2}, N_{E2}, N_{F2}]\\ N_{m3} &= [N_P, N_Q, N_R, N_S]\end{aligned} \tag{25}$$

For convenience, the subscripts $m1$, $m2$ and $m3$ will indicate quantities calculated in the points (A1, B1, C1, D1, E1, F1), (A2, B2, C2, D2, E2, F2) and (P, Q, R, S), respectively. Therefore, the strain components are interpolated as follows:

$$\begin{aligned}\boldsymbol{\varepsilon}_p &= \begin{bmatrix}\varepsilon_{11}\\ \varepsilon_{22}\\ \varepsilon_{12}\end{bmatrix} = \begin{bmatrix}N_{m1} & 0 & 0\\ 0 & N_{m2} & 0\\ 0 & 0 & N_{m3}\end{bmatrix}\begin{bmatrix}\varepsilon_{11_{m1}}\\ \varepsilon_{22_{m2}}\\ \varepsilon_{12_{m3}}\end{bmatrix}\\ \boldsymbol{\varepsilon}_n &= \begin{bmatrix}\varepsilon_{13}\\ \varepsilon_{23}\\ \varepsilon_{33}\end{bmatrix} = \begin{bmatrix}N_{m1} & 0 & 0\\ 0 & N_{m2} & 0\\ 0 & 0 & 1\end{bmatrix}\begin{bmatrix}\varepsilon_{13_{m1}}\\ \varepsilon_{23_{m2}}\\ \varepsilon_{33}\end{bmatrix}\end{aligned} \tag{26}$$

where the strains $\varepsilon_{11_{m1}}$, $\varepsilon_{22_{m2}}$, $\varepsilon_{12_{m3}}$, $\varepsilon_{13_{m1}}$, $\varepsilon_{23_{m2}}$ are expressed by means of Eq.s (24), in which the shape functions N_i are calculated in the tying points. More details about the MITC9 shell element are given in [16].

3 NUMERICAL RESULTS

The Scordelis-Lo barrel vault problem is addressed in this paper in order to carry out performance comparisons of the proposed 1D and 2D formulations. Figure 4 shows the geometry of the structure and Table 1 presents the main characteristics of the model, more details about this problem can be found in [27].

Table 2 presents the results obtained, transverse displacements are considered. First-order Shear De-

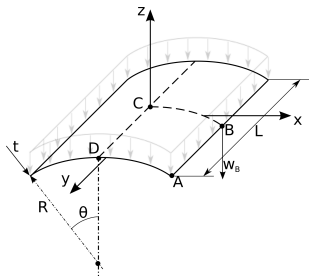

Figure 4: Geometry of the barrel vault.

Barrel vault		
Young's modulus	E	4.32×10^8 lb/ft^2
Poisson's ratio	ν	0.0
load	P	90 lb/ft^2
length	L	50 ft
radius	R	25 ft
thickness	t	0.25 ft
angle	θ_0	$2\pi/9$ rad

Table 1: Physical data of the barrel vault.

formation Theory (FSDT), first-order (ESL1) and second-order (ESL2) shell models were exploited. 1D models up to the fifth-order (TE5) were used. A $20X20$ mesh was used for the shell model (nine-node element) whereas a 20 B4 mesh was used for the 1D model. The total number of degrees of freedom (DOFs) is indicated per each model. It has to be underlined that the shell solution was obtained by considering only a quarter of the structure whereas the 1D model considered the whole structure. The FSDT solution was obtained also without the membrane locking correction. Figure 5 shows the 3D deformed configuration of the barrel vault obtained by means of the TE5 1D model.

These results suggest the following:

1. An excellent agreement with the reference solution was found by means of both the shell and beam formulation.
2. As far as the shell model is concerned, an FSDT model is enough for the result convergence. The membrane locking correction is beneficial.
3. A fifth-order beam model is instead necessary to obtain satisfactory accuracies.
4. The 1D formulation proposed is able to detect the shell solution with some 15 times lower computational costs.

2D shell			
Model	w [ft]	DOFs	$Error^{**}$
FSDT	0.30104	8045	-0.45%
FSDT*	0.30098	8045	-0.47%
ESL1	0.30104	10086	-0.45%
ESL2	0.30104	15129	-0.45%
1D beam			
TE1	0.01869	549	-94%
TE2	0.02631	1089	-91%
TE3	0.11364	1830	-62%
TE4	0.25127	2745	-17%
TE5	0.30335	3843	$+0.31\%$

$(*)$: Without membrane locking correction.

$(**)$: Reference value: $w = 0.3024[ft]$ [27]

Table 2: Barrel vault transversal displacement at point B of the midsurface.

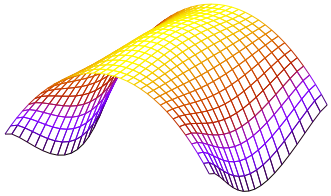

Figure 5: Barrel vault 3D deformation, TE5 1D model.

4 CONCLUSIONS

This paper has presented comparisons between higher-order beam and shell solutions for the barrel vault problem proposed by Scordelis and Lo. The 1D and 2D formulations presented have been derived in the framework of the Carrera Unified Formulation (CUF) which considers the order of a structural model as an input of the analysis. Numerical examples have been carried out in order to investigate the accuracy issues of the models and their computational costs. The following remarks can be stated:

1. CUF models are reliable and compact tools which can be used for a large variety of structural problems.

2. The adoption of higher-order 1D models make the typical limitations of classical models disappear. Particularly powerful is the CUF capability of considering the order of the model as an input, this allows the detection of the exact solution via a convergence study.

3. 1D CUF models detect shell-like solutions with considerable reductions of computational costs and without some typical issues of shell models such as the membrane locking.

Future works should include studies on pinched cylinders, composite structures and free-vibration analyses.

ACKNOWLEDGMENTS

The Regione Piemonte project MICROCOST is gratefully acknowledged for the financial support.

References

[1] L. Euler, *De Curvis Elasticis* Bousquet, Lausanne and Geneva, (1744).

[2] S.P. Timoshenko, "On the corrections for shear of the differential equation for transverse vibrations of prismatic bars," *Philosophical Magazine*, **41**, 744-746, (1921).

[3] K. Kapania and S. Raciti, "Recent advances in analysis of laminated beams and plates, part I: Shear effects and buckling," *AIAA Journal*, **27**(7), 923-935, (1989).

[4] W.T. Koiter, "On the foundations of the linear theory of thin elastic shell," in *Proc. Kon. Nederl. Akad. Wetensch.*, **73**, 169-195, (1970).

[5] P.M. Naghdi, "The theory of shells and plates.", *Handbuch der Phisik*, **6**, 425-640, (1972).

[6] H. Hakula, Y. Leino and J. Pitkäranta, "Scale resolution, locking, and higher-order finite element modelling of shells", *Computer Methods in Applied Mechanics and Engineering*, **133**, 155-182, (1996).

[7] C. Chinosi, L. Della Croce and T. Scapolla, "Hierarchic finite elements for thin Naghdi shell model", *International Journal of Solids and Structures*, **35**, 1863-1880, (1998).

[8] 0.C. Zienkiewicz, R.L. Taylor and J.M. Too, "Reduced integration techniques in general analysis of plates and shells", *International Journal for Numerical Methods in Engineering*, **3**, 275-290, (1971).

[9] H. Stolarski and T. Belytschko, "Reduced integration for shallow-shell facet elements", in *New Concepts in Finite Element Analysis*, ed. by T.J.R. Hughes, et. al., ASME, New York, 179-194 (1981).

[10] J.J. Rhiu and S.W. Lee, "A new effcient mixed formulation for thin shell finite element models", *International Journal for Numerical Methods in Engineering*, **24**, 581-604, (1987).

[11] C. Chinosi, L. Della Croce and T. Scapolla, "Solving thin Naghdi shells with special finite elements", *Mathematical Modelling and Scientific Computing*, **8**, (1997).

[12] E. Carrera, "Theories and finite elements for multilayered plates and shells: a unified compact formulation with numerical assessment and benchmarking", *Arch Comput Methods Eng*, **97**, 10-215, (2003).

[13] E. Carrera, "Multilayered Shell Theories that Account for a Layer-Wise Mixed Description. Part II. Numerical Evaluations", *AIAA Journal*, **37**, 1117-1124, (1999).

[14] D. Chapelle and K.J. Bathe, "*The finite element analysis of shells. Fundamentals.*", Springer, Berlin, (2003).

[15] C. Chinosi and L. Della Croce, "Mixed-interpolated elements for thin shell", *Communications in Numerical Methods in Engineering*, **14**, 1155-1170, (1998).

[16] M. Cinefra, C. Chinosi and L. Della Croce, "MITC9 shell elements based on refined theories for the analysis of isotropic cylindrical structures", *Mechanics of Advanced Materials and Structures*, (2011), in press.

[17] E. Carrera and G. Giunta, "Refined beam theories based on a unified formulation", *International Journal of Applied Mechanics*, **2**(1), 117-143, doi: 10.1142/S1758825110000500, (2010).

[18] E. Carrera, G. Giunta and M. Petrolo, "A Modern and Compact Way to Formulate Classical and Advanced Beam Theories", In: *Developments in Computational Structures Technology*, Ch. 4, DOI: 10.4203/csets.25.4, (2010).

[19] E. Carrera, G. Giunta, P. Nali and M. Petrolo, "Refined beam elements with arbitrary cross-section geometries", *Computers and Structures*, **88**(5-6), 283-293, doi: 10.1016/j.compstruc.2009.11.002, (2010).

[20] E. Carrera, M. Petrolo and E. Zappino, "Performance of CUF approach to analyze the structural behavior of slender bodies", *Journal of Structural Engineering*, doi:10.1061/(ASCE)ST.1943-541X.0000402, In press.

[21] E. Carrera, M. Petrolo and P. Nali, "Unified formulation applied to free vibrations finite element analysis of beams with arbitrary section", *Shock and Vibrations*, **18**(3), 485-502, doi: 10.3233/SAV-2010-0528, (2011).

[22] E. Carrera, M. Petrolo and A. Varello, "Advanced Beam Formulations for Free Vibration Analysis of Conventional and Joined Wings", *Journal of Aerospace Engineering*, doi:10.1061/(ASCE)AS.1943-5525.0000130, In Press.

[23] E. Carrera and M. Petrolo, "On the Effectiveness of Higher-Order Terms in Refined Beam Theories", *Journal of Applied Mechanics*, **78**(4), doi: 10.1115/1.4002207, (2011).

[24] E. Carrera and M. Petrolo, "An Advanced One-Dimensional Formulation for Laminated Structure Analysis", *AIAA Journal*, In Press.

[25] K.J. Bathe and E. Dvorkin, "A formulation of general shell elements - the use of mixed interpolation of tensorial components", *International Journal for Numerical Methods in Engineering*, **22**, 697-722, (1986).

[26] M.L. Bucalem and K.J. Bathe, "High-order MITC general shell elements", *International Journal for Numerical Methods in Engineering*, **36**, 3729-3754, (1993).

[27] A.C. Scordelis, K.S. Lo, "Computer analysis of cylindrical shells", *J. Am. Concr. Inst.*, **61**, 539-560, (1964).